MATERIALS TECHNOLOGY
2020, VOL. 35, NO. 4, 238–247
https://doi.org/10.1080/10667857.2019.1674506

Taylor & Francis
Taylor & Francis Group

Surface characterization, biocompatibility and osteogenic differentiation of drop-casted multilayer graphene oxide film towards human wharton's jelly derived mesenchymal stem cells

Perng Yang Puah [a,b], Umul Hanim Yusoff [a,c], Ping Chin Lee [a], Pak Yan MOH [b] and Siew Eng How [b]

[a]Programme of Biotechnoology, Faculty of Science and Natural Resources, Universiti Malaysia Sabah, Kota Kinabalu, Malaysia;
[b]Programme of Industrial Chemistry, Faculty of Science and Natural Resources, Universiti Malaysia Sabah, Kota Kinabalu, Malaysia;
[c]Biotechnology Research Institute, Universiti Malaysia Sabah, Kota Kinabalu, Malaysia

ABSTRACT

Graphene oxide (GO) materials have been extensively employed in mesenchymal stem cell (MSCs) research due to its unique nanotopography. Herein, various concentrations of GO flakes were used to fabricate different thickness of multilayer graphene oxide (m-GO) films using a simple drop-casting method and characterized by FTIR and AFM. The biocompatibility of m-GO films in culturing WJ-MSCs was investigated based on cell morphology, cell viability and osteogenic differentiation ability. Importantly, WJ-MSCs adhered and proliferated successfully on the m-GO films (6.25 µg, 12.5 µg and 25 µg) and showed no difference in cell morphology and viability after 5 days culture. Moreover, the WJ-MSCs growth on GO films (6.25 µg, 12.5 µg and 25 µg) enhanced the osteogenic differentiation as compared to the control (glass coverslip). Hence, the simple and inexpensive drop-casted fabrication strategy could provide biocompatible m-GO films to unlock the wider potential of WJ-MCSs in tissue engineering application.

ARTICLE HISTORY
Received 19 July 2019
Accepted 24 September 2019

KEYWORDS
Multilayer Graphene oxide; drop-casted self-assembling; surface characterization; Wharton's Jelly mesenchymal stem cell; cell differentiation

Introduction

Human umbilical cord has been collected and used as an alternative source of stem cells. Mesenchymal stem cells isolated from the umbilical cord are noninvasive, do not turn into carcinogenic or teratogenic cells during transplantation [1–3]. Mesenchymal stem cells (MSCs) isolated from a mucilaginous jelly-like substance (Wharton's jelly) within the human umbilical cord are referred as Wharton's jelly mesenchymal stem cells (WJ-MSCs). WJ-MSCs show a higher capacity of ex vivo expansion and shorter doubling time in terms of proliferation as compared to the bone marrow isolated MSCs (BM-MSCs) [4,5]. For the past decades, several studies have reported the differentiation potential of WJ-MSCs into adipogenic, osteogenic, chondrogenic, angiogenic, neurogenic and myogenic [6–9]. In the year 2014 itself, several papers reported that umbilical cord matrix-derived mesenchymal stem cells (UC-MSCs) can express markers of male germ-like cells and primordial-like germ cells under specific conditions [10,11]. This proves that WJ-MSCs may have similarity to embryonic stem cells (ESCs) or induced pluripotent stem cells (iPSCs). However, WJ-MSCs have poor osteogenic and chondrogenic potential as compared to BM-MSCs [12,13].

The combination of WJ-MSCs with scaffold materials offers a promising strategy for regulating or improving the WJ-MSCs function in cell therapy and tissue engineering applications [14,15]. A study by Hosseini *et al.* (2015) demonstrated that WJ-MSCs cultured in 3D alginate scaffold under neurogenic medium expressed higher levels of both neuron and motor neuron markers than the 2D alginate scaffold condition. This finding shows that the alginate stiffness can influence the neurogenic differentiation capability of WJ-MSCs [16]. Recently, enhanced osteogenic differentiation was observed when WJ-MSCs being cultured into 3D nanoscaffolds: polycaprolactone-collagen-hydroxyapatite (PCL-Coll-HA) nanofibers [17]. The nanoscaffolds formed by three different materials have the suitable properties for WJ-MSCs because PCL is a substance used as a bone substitute. The HA closely resembles natural bone and collagen I which are the organic components of bone extracellular matrix (ECM). This study shows that mimicking the structural and bio-chemical cues like ECM may provide a suitable environment for cells to attach, proliferate and thus enhance the differentiation lineage [17].

Various external stimulations of scaffolds have shown their involvement in directing the differentiation of WJ-MSCs into several lineages [16–18]. Thus, the key components can be controlled through different engineering approaches to mimic the cell microenvironment that can further enhance and direct the stem cell fate. Graphene-based research was awarded a Noble Prize in physics recently, 2010 for Andre Geim and Kostya Novoselov

CONTACT Siew Eng How sehow@ums.edu.my; Pak Yan Moh pymoh@ums.edu.my Programme of Industrial Chemistry, Faculty of Science and Natural Resources, Universiti Malaysia Sabah, Jalan UMS, 88400 Kota Kinabalu, Sabah, Malaysia
Supplemental data for this article can be accessed here

due to their groundbreaking experiment related to the 2D material-Graphene [19,20]. Since then, graphene-based materials have been studied extensively for various applications, including sensors, nanoelectronics, energy storage, nanocarriers for drug, nanocomposites and so on [21–26]. Recently, graphene oxide (GO) materials have been applied to tissue engineering and induction of stem cell differentiation due to the unique physical framework and surface functional groups that can modulate the stem cell behaviours [27–30].

In our previous study, we found that WJ-MSCs cultured on a spin-coated GO substrate demonstrate promising cell viability for at least six days and this result is comparable to WJ-MSCs grown on a glass substrate (without GO) [31]. However, we noticed that the spin-coated GO substrate was not fully covered by GO. Under spin coating method, the WJ-MSCs were adhered to the mix surfaces of glass coverslip and GO. The surface topography of any biomaterial is a vital parameter that influences the cell-material interaction [32,33]. Thus, in this current study, we intended to investigate the biocompatibility of WJ-MSCs on a total GO surface. To achieve the aim, GO flakes were self-assembly through a drop-casted method forming multilayer graphene oxide (m-GO) films in which the glass substrate support was fully covered. We hypothesized that the m-GO films could offer a suitable environment for culturing WJ-MSCs. This scaffold coating can be used for future tissue engineering application of WJ-MSCs.

Experimental

Fabrication of multilayer graphene oxide (m-go) film

Graphene oxide (GO) and pre-treatment of glass coverslips (diameter of 10 mm, thickness of 0.13 mm-0.16 mm, circular shape) (L46R10–1, Agar Scientific Limited, Stansted, UK) were prepared according to our previously reported method [31,34]. Briefly, graphite flakes (1.00 g, Sigma-Aldrich®) and $KMnO_4$ (6.00 g, 99%, Merck) were mixed with H_2SO_4 (120.00 mL, 95–97%, QRëC®) and H_3PO_4 (13.30 mL, 85%, Systerm® ChemPur®). The suspension was stirred at 50°C for 24 h. The reaction was then cooled to room temperature and a mixture of ice water (400.00 mL) and H_2O_2 (8.00 mL, 30%, J.T.Baker®) was added. The suspension was centrifuged at 4000 rpm for 5 minutes. The remaining solid material was then washed with HCl (37%, Fisher Scientific), deionized water and then sonicated for 60 minutes to obtain graphene oxide (GO) solution. The solution was then freeze-dried (Labconco, Kansas City, MO, USA) to obtain GO flakes. On the other hand, 10-mm glass coverslips (100 pieces) were cleaned by immersing into a piranha solution (50.00 mL, a mixture of hydrogen peroxide (H_2O_2)/sulfuric acid (H_2SO_4), 1:3 ratio, v/v) for 15 min at 120°C, followed by rinsing with ethanol (50.00 mL, 96%, Merck) and distilled water (50.00 mL). The cleaned coverslips were then pre-treated with 50.00 mL of 3% of 3-aminopropyltriethoxysilane (3-APTES) (99%, Sigma-Aldrich®) in toluene (99%, Merck) solution for 30 min. The substrate was then washed with toluene (50.00 mL), ethanol (50.00 mL X 2), distilled water (50.00 mL X 2) and annealed at 110°C for 20 minutes.

The GO film substrates were fabricated through the drop-casting method as previously reported [35] with a minor modification. In detail, GO flakes were dispersed in distilled water by sonication for 2 h, at concentration of 0.0625 mg/mL, 0.125 mg/mL, 0.25 mg/mL, 0.50 mg/mL and 1.0 mg/mL. Then, GO dispersions (100 µL of each of the concentration) were added to the treated coverslip and allowed to dry at 30°C for 24 h. Finally, multilayer graphene oxide films (m-GO films) coated on glass coverslips fabricated with different loading amounts of GO (6.25 µg, 12.5 µg, 25 µg, 50 µg and 100 µg) were obtained. Figure 1 shows the schematic diagram of drop-casting preparation of m-GO films.

Characterization of m-go films

Both non-coated and m-GO films coated glass substrates were analyzed using Perkin-Elmer Spectrum 100 Fourier transform infrared spectroscope (FTIR) to evaluate the changes of functional groups. While the morphology characterization of m-GO films was evaluated using a Bruker Dimension Edge atomic force microscopy (AFM) coupled with ScanAsyst-Air cantilevers at 0.4 N/m nominal spring constant. The measurement of the film's thickness and surface roughness was calculated by NanoScope Analysis 1.7 software.

Cell culture

This study was approved by the Ethics and Research Committee, Universiti Malaysia Sabah with an approval code: JKEtika 1/16 (1). The Human Wharton's Jelly Mesenchymal Stem Cells (WJ-MSCs) from umbilical cord matrices were kindly given by Dr. Siti Fatimah Simat. The given WJ-MSCs were maintained as in our previous report [31].

All the cell assays on fabricated films were carried out using WJ-MSCs at between passages 3 to 5. The m-GO films (n = 3) were sterilised with UV for 20 min prior to cellular studies. The m-GO films coated on 10-mm glass coverslips were placed into a 48-well plate with 10,000 WJ-MSCs cells seeded in each of the wells. Prior to cell seeding on samples, a cell count was performed using a Haemacytomer, and a standard culture medium Dulbecco's modified Eagle's medium: Nutrient Mixture F-12 (350 µL, DMEM/F-12) (Gibco, UK) supplemented with 10% FBS (Gibco, UK), 1% antibiotic-antimycotic (Gibco, UK), 1% Glutamine (Gibco, UK) and 1% L-ascorbic

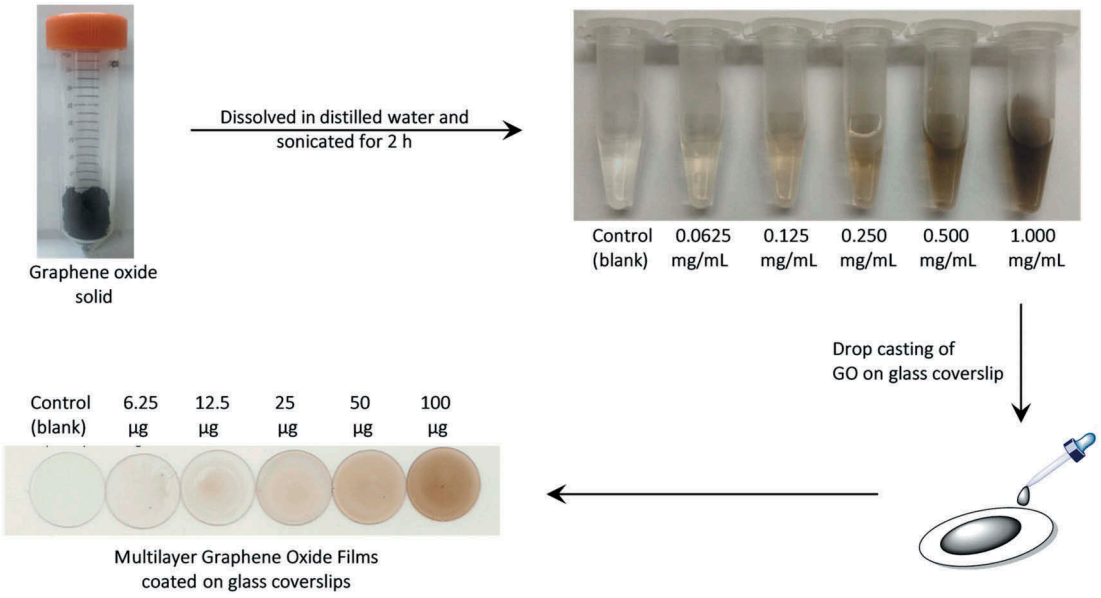

Figure 1. Schematic diagram of fabrication of m-GO films with five different concentrations of GO flakes dispersions through a drop-casting method. The blank glass coverslip serves as a control.

acid (Sigma, USA) was added to each well for cell proliferation and incubated at 37°C in a humidified 5% CO_2. The media were changed every three days. Cells seeded directly on a blank glass coverslip on the 48-well plate served as the control and cell viability at Day 5 incubation was determined by a MTT assay.

Cell viability assay

Methylthiazolyldiphenyl-tetrazolium bromide (MTT) (≥97.5%, Sigma-Aldrich®, USA) assay was used to determine the cell viability of WJ-MSCs growth on the films. After 5 days of incubation, the medium was removed and the colourimetric tetrazolium MTT (200 µL, 0.5 mg/mL) was added to each well and incubated at 37°C for 2 hours for a cell response to take place. The formazan precipitates reduced by the living cells in each well were suspended by dimethyl sulfoxide (200 µL, ≥99.9%, Merck, Germany). The culture plate was then wrapped with aluminium foil and gently shaken using a Mini Rocker MR-1 shaker (Biosan, Latvia) for 10 min at room temperature. Then, the resulting solution (100 µL) was transferred into a new 96-well plate and optical density, at 570 nm, was measured using the Infinite M200Pro microplate reader (TECAN, Austria). Results were prior normalized with Blank control (50 µL of MTT solution + 50 µL of cell culture media without cells). The percentage of cell viability (%) cultured on m-GO films was reported by comparing to the control (non-coated coverslip) calculated as $\frac{sample}{control(non-coated\ coverslip)} \times 100\%$.

Cell morphology

The morphology of the WJ-MSCs on all the surfaces was observed by using an inverted microscope (Olympus IX73, Japan). Prior to viewing by the microscope, cell medium was discarded, and cells were washed with 1x phosphate-buffered saline (200 µL, PBS). The images of WJ-MSCs incubated on films under the desired incubation period, were captured with either 4x, 10x or 40x magnification. For nucleus observation, the WJ-MSCs were stained with NucBlue® Fixed Cell Stain ReadyProbes™ Reagent (DAPI, Life Technologies). The fluorescent microscopy images were captured using an inverted fluorescent microscope (Olympus IX73, Japan) with CellSens software (Olympus, Japan) employed.

To observe the proliferated WJ-MSCs adhered to the fabricated biomaterials, the WJ-MSCs were fixed with a modified Karnovsky's fixative consisting of 2% paraformaldehyde (Sigma-Aldrich, USA) and 2% glutaraldehyde (Sigma-Aldrich, USA) in a 1x PBS (350 µL) for overnight at 4°C. This protocol was adapted from a previously reported method [27]. After fixation, cells were washed with 1x PBS (200 µL) three times for 10 min. The cells were then washed with distilled water (200 µL) and dehydrated sequentially in 50%, 70%, 80%, 90%, and 100% absolute ethanol (200 µL of each of the concentration, ≥99.8%, VWR Chemical Prolabo®). Before imaging, the fixed cells were treated with hexamethyldisilazane (HMDS, Ted Pella Inc, Redding, CA, USA) for 15 min. Finally, the dried cells were coated with platinum using a sputter-coater (JFC-1100E, JEOL) and cells adhered to biomaterials were observed by SEM (JEOL, JSM-5610LV, Japan).

Osteogenic differentiation

To induce the osteogenic differentiation of WJ-MSCs on the control (glass) and m-GO films, WJ-MSCs were seeded at a density of 10,000 cells/well (n = 3) in the

standard culture medium. After 3 days, the standard culture medium was then replaced with StemPro osteogenesis differentiation kit (Invitrogen, cat. no. A1007201) according to manufacturer direction. The induction medium was changed every 2–3 days and cultures were continued for 14 days. The cells were then washed with 1x PBS (300 µL) once and fixed in 10% formalin in PBS (300 µL), for 20 min at room temperature. After fixation, the well plate was washed three times with 1x PBS (300 µL) and once with distilled water (300 µL). Osteogenic induced cells were stained with Alizarin red solution Kit (Invitrogen, USA). Prior to observing under an inverted microscope (Olympus IX73, Japan), samples were washed with distilled water three times (300 µL).

Statistical analysis

Numeric data were presented as mean ± standard error of the mean (SEM). The significant differences existed between mean values of those experimental groups for MTT assay (n = 3) were analyzed using a one-way analysis of variance (ANOVA) followed with t-test and considered significant with $p < 0.05$.

Results and discussion

Characterization of m-go films

FT-IR spectra of non-coated and m-GO film coated on glass substrate are displayed in Figure 2. No peaks were observed between 1500–4000 cm^{-1} for non-coated glass substrate. However, several peaks were observed for the m-GO film coated on the glass substrate. A broad peak at 3390 cm^{-1} (O-H vibration) shows the hydroxyl group of the GO. A characteristic peak observed at 1739 cm^{-1} for the C = O stretching belonging to the oxidized carboxyl group on the graphene surface. Typical stretching bands of GO at 1629 cm^{-1} observed on the m-GO film belonging to the C = C stretching. The FTIR analysis of m-GO films spectrum demonstrated the successful fabrication of m-GO film onto the glass substrate without interfering the main functional group of GO flakes [31,36].

To examine the surface characterization of glass (control) and m-GO films substrate, the topography was first measured using AFM in height image (Figure 3(a–f)). Then, m-GO films were scratched along the radius and the step height was measured by AFM (Fig. S2) to determine the thickness of the m-GO film (Figure 3 (g)). Based on the AFM height images (Figure 3(a–f)), the GO flakes were randomly self-assembled on one another, and no special pattern was observed. However, 'hills' and 'valleys' with a height of lower than 60 nm can be observed (Fig. S1) and eventually formed wrinkle morphology on the surface of m-GO films. The formation of such morphology is due to amphiphilicity of GO flakes which homogenously distributed in the water and due to the continuous water evaporations, the multilayer GO films start to form by self-assembling of small GO flakes at the water-air interface [37,38]. As a result of water evaporates slowly, the GO flakes start to stack over one another and appear to be wrinkled surface. The surface roughness (mean-square roughness, Rq) and thickness of all prepared substrates including the glass (control) and various m-GO films prepared by different loading amounts of GO flakes (6.25 µg, 12.5 µg, 25 µg,

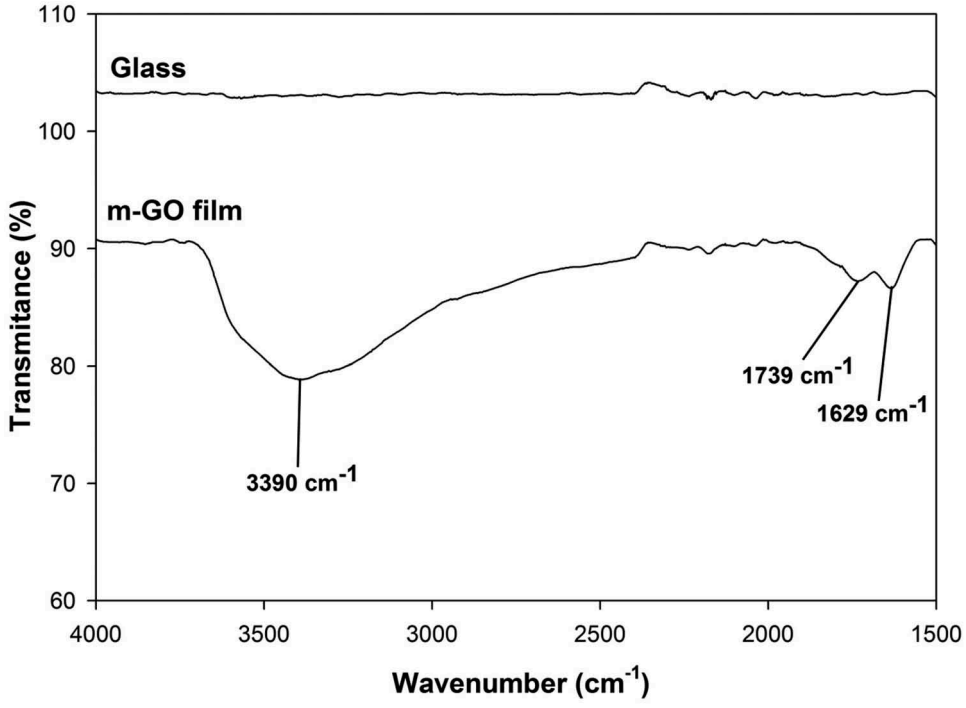

Figure 2. FT-IR spectra of glass coverslip (top) and m-GO film (bottom).

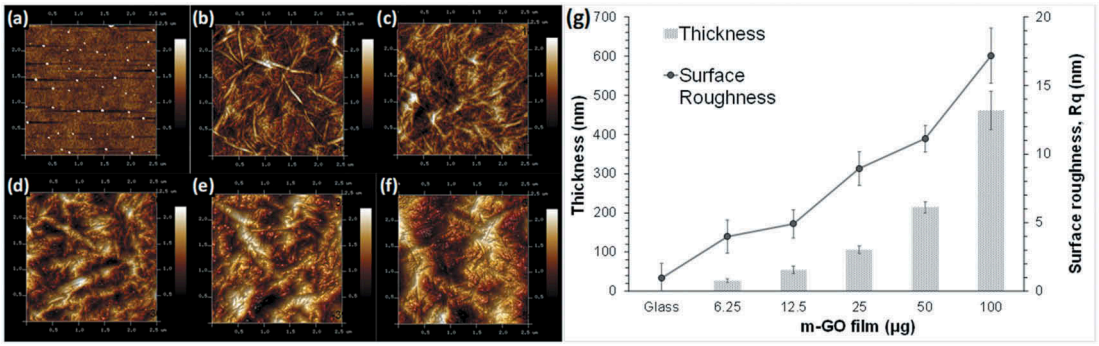

Figure 3. AFM height images: (a) Glass coverslip (control), (b) m-GO film (6.25 µg), (c) m-GO film (12.5 µg), (d) m-GO film (25 µg), (e) m-GO film (50 µg) and (f) m-GO (100 µg). Image sizes are all 2.5 × 2.5 μm^2. (g) The surface roughness and the mean thickness of m-GO films.

50 µg and 100 µg) were measured from the height profile of the AFM images (Figure 3(a-f) and Fig. S2). Results depict that (Figure 3(g)), all the m-GO film-coated substrates possess rougher surface as compared to the glass substrate (control). As the concentration of GO flakes solution increased, both the surface roughness and the mean thickness of m-GO films increased gradually due to the higher loading amount of GO flakes. Among the prepared m-GO films, the highest surface roughness was 17.17 ± 2.01 nm which was m-GO film (100 µg), while the mean thickness was about 461.20 ± 48.75 nm equivalent to about 460 layers of single GO sheet stacked over one another [31]. Besides, the m-GO film (6.25 µg) possessed the lowest surface roughness (3.99 ± 1.19 nm) among all m-GO films prepared and the mean thickness was about 27.05 ± 4.66 nm equivalent to about 27 layers of single GO sheet. Using this deposition method, the higher the amount of GO flakes deposited on the glass, the thicker the multilayer of GO with surface roughness increases accordingly. These results reveal the surface characteristic and confirm the successful formation of the m-GO films with different amounts of GO flakes loading on the glass substrate as support.

Wj-mscs viability and morphology on the m-go films

To determine whether the different loading amount of m-GO films gives a significant effect on the WJ-MSCs, MTT assay was performed to identify the cell viability on m-GO films drop casted with different loading amounts of GO flakes (6.25 µg, 12.5 µg, 25 µg, 50 µg and 100 µg) while the glass coverslip (without GO coated) was used as a control. Figure 4 shows the cell viability after 5 days of cell culture on the m-GO films respectively. Although the glass (control) showed slightly higher cell viability, there was no significant difference ($p > 0.05$) of cell viability on m-GO films with lower loading amounts of GO flakes (6.25 µg, 12.5 µg and 25 µg) was observed as compared to the control. These m-GO films (6.25 µg, 12.5 µg and 25 µg) could potentially stimulate interaction between cells and the materials, which may result in a suitable condition for cell adhesion and regeneration. However, a significant difference ($p < 0.05$) of cell viability was noted on m-GO films with higher loading amounts of GO flakes (50 µg and 100 µg) as compared to the control. There were some discrepancies with early work reported by Rosa and co-workers, where a similar drop-casted GO film prepared by 250 uL with 1.5 mg/mL GO flakes solution (equivalent to 375 µg) on coverslip (22 mm × 22 mm) to culture dental pulp stem cells (DPSC). Their results show similar cell proliferation as compared to control (glass) at day 5 [35]. The differences in GO characterizations and sources of stem cells could explain these discrepancies [30,39,40].

The MTT results are in good agreement with the observation of WJ-MSCs attached to the m-GO films (Figure 5). WJ-MSCs cultured on the control (glass coverslip) and m-GO films (6.25 µg, 12.5 µg and 25 µg) were homogeneously dispersed on the surface which reached 80% confluency. However, WJ-MSCs cultured on m-GO films (50 µg and 100 µg) appeared to have fewer attached cells and shorter cells as compared to other substrates. All the WJ-MSCs cultured in both control and m-GO films displayed spindle-shaped and fibroblast-like morphology, which is the typical morphological characteristic of WJ-MSCs [41]. Due to the thin layer of m-GO films coated on the coverslips, the attachment and growth of WJ-MSCs on the surface GO biofilm (25 µg) was further studied by observing using SEM. The higher magnification images (Figure 6) show that WJ-MSCs attached to the m-GO film where the cells seen to adhere with flattened morphology and successfully anchored to the rough surface provided by m-GO film with cellular microextensions. Moreover, WJ-MSCs growth on both control (glass coverslip) and m-GO film possess a similar cell morphological characteristic suggesting their high adaptation with the surface of m-GO film.

The cell viability and morphological characterization successfully show the biocompatibility of the m-GO films (6.25 µg, 12.5 µg and 25 µg). To further explore the

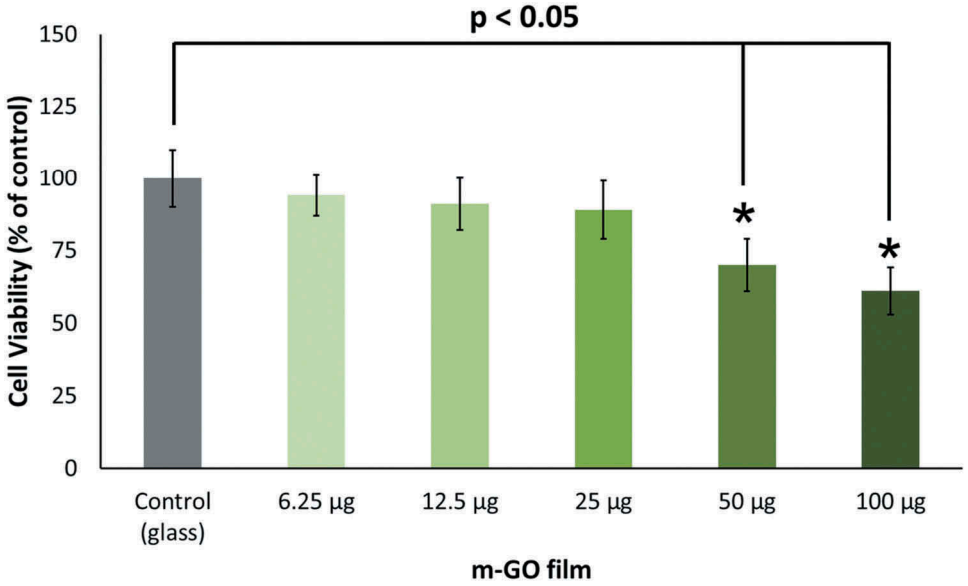

Figure 4. Cell viability of the WJ-MSCs cultured on all the m-GO films (6.25 µg, 12.5 µg, 25 µg, 50 µg and 100 µg) at Day 5 was quantified by MTT assay. The bar chart plotted by results normalized with the control (glass coverslip), which was taken as 100%. Three independent experiments performed in replicates were conducted using single isolated WJ-MSCs between passages 3–5 and the error bars represent the SD about the mean. Asterisk (*) indicates a statistical significance compared to control glass coverslip ($n = 3$, $p < 0.05$).

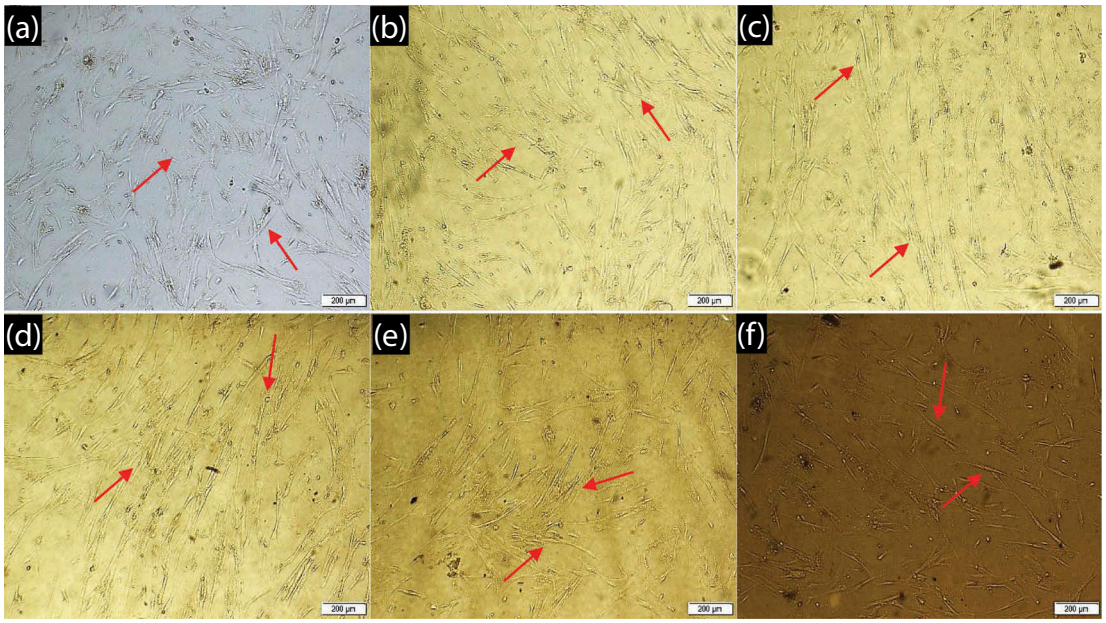

Figure 5. Micrographs showing WJ-MSCs cells attachment and growth on all the studied surfaces at Day 5. (a) Control (glass coverslip), (b) m-GO film (6.25 µg), (c) m-GO film (12.5 µg), (d) m-GO film (25 µg), (e) m-GO film (50 µg) and (f) m-GO (100 µg). All scale bars represent 200 µm.

cellular behaviour on m-GO films, cellular nuclei were stained by DAPI to trace morphological alteration, for example, shrinkage of the cell, chromatin condensation, and nuclear fragmentation [42,43]. As shown in Figure 7, most of the cells from both control (glass coverslip) and m-GO (25 µg) appeared big and regular nuclei. According to Ryoo and co-workers, their studies suggest that high gene transfection efficiency (>250%) of standard mouse embryonic fibroblast cell line (NIH-3T3) grown on GO surface [44]. Indeed, Kang et al reported that large miro-size of GO sheets enables enhanced cell spreading and proliferation of human adipose-derived MSCs as compared to nano-size GO sheet [45]. This may explain the m-GO film prepared in this study did not hamper the attachment and growth of WJ-MSCs, and a good control of GO flakes loading (≤25 µg) is able to provide a suitable environment for the proliferation of WJ-MSCs. Cell attachment and proliferation are directly correlated with the physico-chemical properties of biomaterials such as hydrophilicity, surface topography, and chemistry. Extracellular matrix will regulate the outcomes of cell surface communicated to intracellular

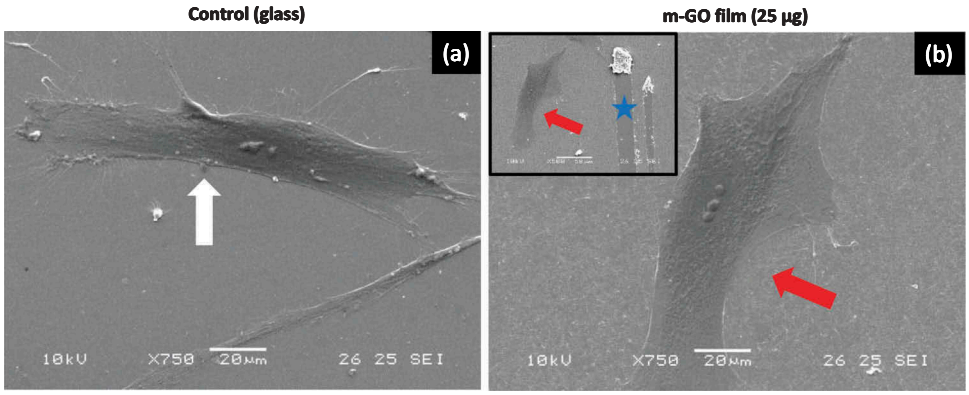

Figure 6. High-magnification SEM images of WJ-MSCs on (a) control (glass coverslip) and (b) m-GO film (25 µg), at Day 3. The white arrow indicates WJ-MSCs adhered to the glass coverslip and red arrows indicate WJ-MSCs adhered to the GO film. The blue star indicates the scratches on the GO film.

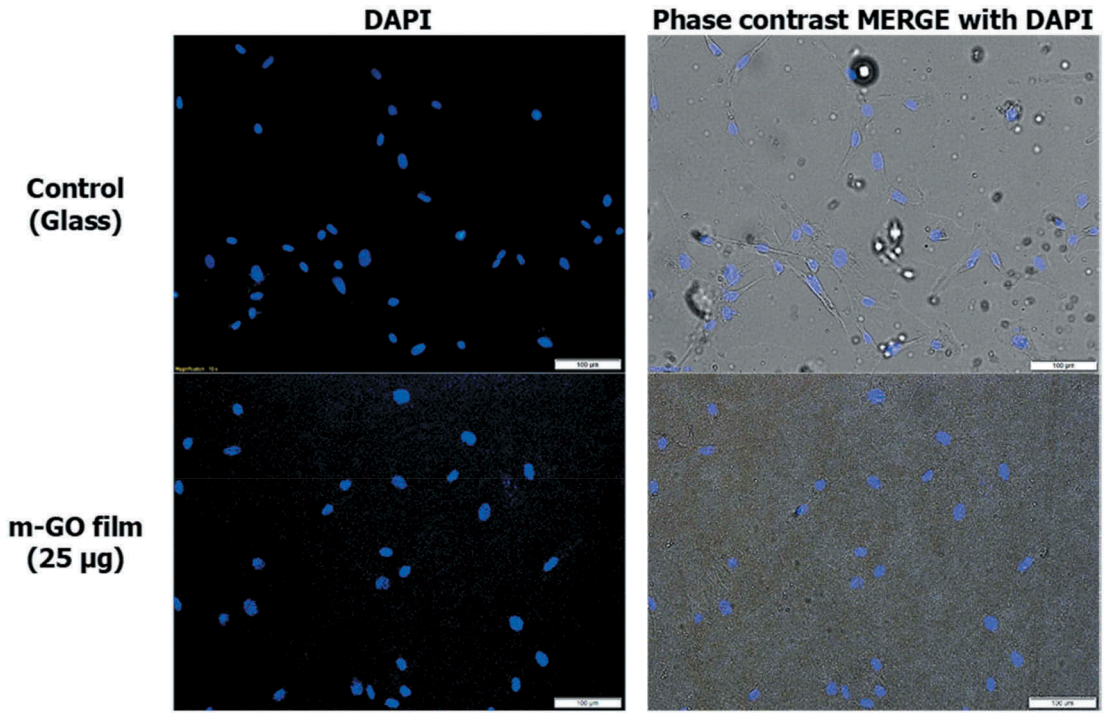

Figure 7. DAPI (blue) stained fluorescent images of WJ-MSCs culture on control (glass coverslip) and m-GO film (25 µg). All scale bars represent 100 µm.

processes through cytoskeletons [46,47]. Thus, the outcomes of cellular and molecular responses towards biomaterials are a cumulative effect of biocompatible graphene oxide, greater hydrophilicity, and surface roughness. The larger the surface area of graphene oxide provides the larger area of binding sites for osteoblast in the hybrid silicon elastomer [47].

Osteogenic differentiation of wj-mscs on the m-go films

Osteogenesis is the major differentiation lineage of MSCs which can be manipulated by the change of GO's physical property [45,48]. Thus, the WJ-MSCs were cultured in m-GO films with different GO flakes loading in osteogenic media and the osteoblast mineralization (calcium deposits) were stained by Alizarin red, which serves as a visual indicator for *in vitro* bone formation [31,45]. By day 14, all the cells cultured in control (glass coverslip) and m-GO films were stained positively with red colour as shown in Figure 8. Notably, red colour staining of calcium deposits of differentiated WJ-MSCs cultured on m-GO films with low loading amounts of GO flakes (6.25 µg, 12.5 µg and 25 µg) are obviously stained than those cultured in control (glass coverslip) and m-GO films with high loading amounts (50 µg and 100 µg). This can be attributed to the surface chemistry of m-GO films which contains aromatic rings that can strongly adsorb with osteogenic chemicals such as dexamethasone, ascorbic acid and β-glycerol phosphate through the π-π interaction [49]. The polar

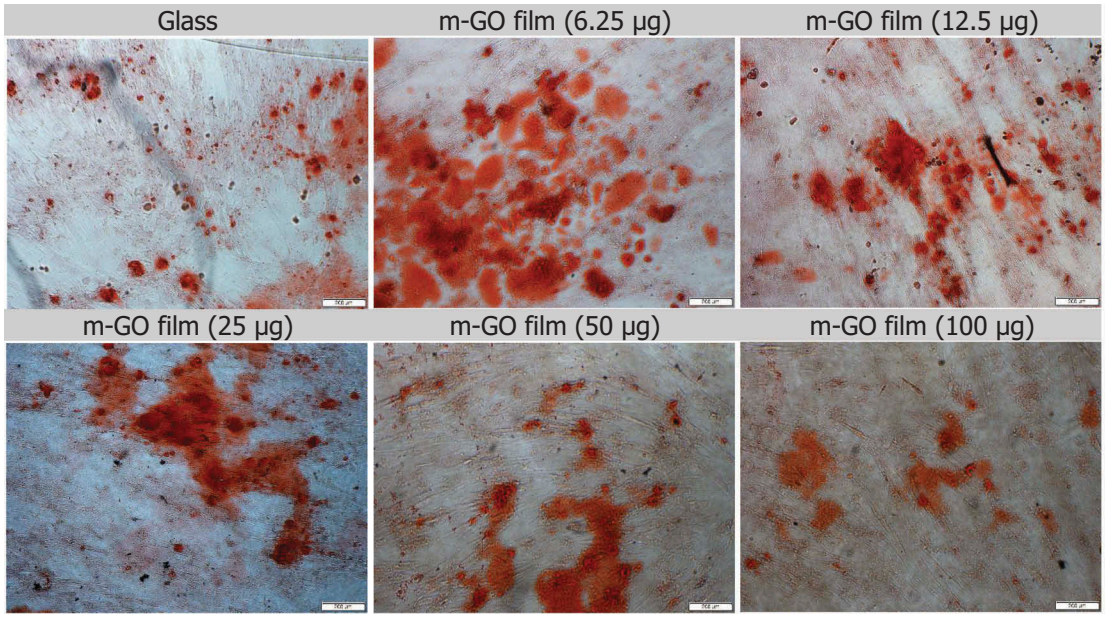

Figure 8. Alizarin red-stained results of WJ-MSCs cultured on control (glass coverslip) and m-GO films for 14 days. All scale bars represent 200 µm.

constituents in a biomaterial play an important role in bone marrow-derived MSCs proliferation and osteogenic differentiation functions. GO contains numerous polar oxygenated groups, namely hydroxyl (OH), epoxy (C-O-C), and carboxyl (COOH) functional groups. Thus, it is likely that various biological substances presence in serum and extracellular matrix proteins are bonded toward the GO substrate via polar forces and electrostatic interactions that create a favorable environment for such biological functions to take place [40]. Less alizarin red staining in m-GO films (50 µg and 100 µg) indicates fewer osteogenic differentiated cell which could be possibly due to the low degree of cell attachment and proliferation of WJ-MSCs [50,51]. The electrostatic interaction and the surface functional groups of GO conjugated with chitosan and hydroxyapatite (HAP) enhance the cellular activities (osteoblast functions: cell attachment, proliferation, actin, vinculin and fibronectin expression) of MC3T3-E1 preosteoblast cells [52]. Therefore, by well controlling the loading amount of GO flakes in the fabrication of m-GO films, a suitable environment for WJ-MSCs proliferation and osteogenic differentiation could be provided. To the best of our knowledge, this study provides the pioneer evidence for the use of drop cast m-GO films as a biomaterial for growing and induce osteogenic differentiation of WJ-MSCs.

Conclusion

In summary, m-GO films fabricated through the self-assembly of GO flakes can be used as biomaterials for culturing WJ-MSCs. The fabricated m-GO films possess similar oxygenated groups as GO flakes. The film thickness and surface roughness increased when a higher amount of GO flakes loaded. The m-GO films with lower loading amounts of GO flakes (6.25 µg, 12.5 µg and 25 µg) showed similar cell growth, maintain cell morphology and enhanced osteogenic differentiation as compared to the control (glass coverslip). As recently graphene-based materials have been widely used for stem cell-based regenerative research, the different loading amount of m-GO films should prior study *in vitro* before the *in vivo* application of such materials. Overalls, the drop casted m-GO films with a low loading amount of GO flakes (6.25 µg, 12.5 µg and 25 µg) could be a promising biomaterial for the future application of WJ-MSCs. Other mechanical properties like modulus of elasticity, tensile strength, fracture toughness, elongation percentage, etc, can be further studied in the near future to correlate the application of using such m-GO film as a biomaterial for growing WJ-MSCs in tissue engineering or regenerative medicine.

Acknowledgments

This work was supported by the Ministry of Higher Education Malaysia through the Transdisciplinary Research Grant Scheme, project no. TRGS001-SG2/2014 and TRGS 0002-SG-2/2014. Special thanks to Dr. Siti Fatimah Simat, Dr. Peik Lin Teoh and their student Miss Warda binti Abdul Ajak for providing the WJMSCs, and Biotechnology Research Institute, UMS for providing the cell culture facilities.

Disclosure statement

No potential conflict of interest was reported by the authors.

Funding

This work was supported by the Ministry of Higher Education Malaysia (MOHE) for the provision of Trans Disciplinary Research Grant Scheme [grant number TRGS0002-SG-2/2014 and TRGS0001-SG-2/2014]

ORCID

Perng Yang Puah http://orcid.org/0000-0002-3032-7376
Umul Hanim Yusoff http://orcid.org/0000-0002-5320-5443
Ping Chin Lee http://orcid.org/0000-0002-4280-0829
Pak Yan MOH http://orcid.org/0000-0002-1974-6481
Siew Eng How http://orcid.org/0000-0003-4002-3736

References

[1] Nagamura-Inoue T, He H. Umbilical cord-derived mesenchymal stem cells: their advantages and potential clinical utility. World J Stem Cells. 2014;6(2):195–202.
[2] Li J, Mao Q, He J, et al. Human umbilical cord mesenchymal stem cells improve the reserve function of perimenopausal ovary via a paracrine mechanism. Stem Cell Res Ther. 2017;8(1):55.
[3] Fong CY, Richards M, Manasi N, et al. Comparative growth behaviour and characterization of stem cells from human Wharton's jelly. Reprod Biomed Online. 2007;15(6):708–718.
[4] Karahuseyinoglu S, Cinar O, Kilic E, et al. Biology of stem cells in human umbilical cord stroma: in situ and in vitro surveys. Stem Cells. 2007;25(2):319–331.
[5] Troyer DL, Weiss ML. Concise review: wharton's jelly-derived cells are a primitive stromal cell population. Stem Cells. 2008;26(3):591–599.
[6] Iwona G, Streminska W, Janczyk-Ilach K, et al. Myogenic potential of mesenchymal stem cells - the case of adhesive fraction of human umbilical cord blood cells. Curr Stem Cell Res Ther. 2013;8(1):82–90.
[7] Aristea KB, Kastrinaki M-C, A. Papadaki H, et al. Mesenchymal stem cells derived from wharton9s jelly of the umbilical cord: biological properties and emerging clinical applications. Curr Stem Cell Res Ther. 2013;8(2):144–155.
[8] Pires AO, Neves-Carvalho A, Sousa N, et al. The secretome of bone marrow and wharton jelly derived mesenchymal stem cells induces differentiation and neurite outgrowth in SH-SY5Y cells. Stem Cells Int. 2014;2014:10.
[9] Xu L, Zhou J, Liu J, et al. Different angiogenic potentials of mesenchymal stem cells derived from Umbilical Artery, Umbilical Vein, and Wharton's Jelly. Stem Cells Int. 2017;2017:1–15.
[10] Li N, Pan S, Zhu H, et al. BMP4 promotes SSEA-1 +hUC-MSC differentiation into male germ-like cells in vitro. Cell Prolif. 2014;47(4):299–309.
[11] Latifpour M, Shakiba Y, Amidi F, et al. Differentiation of human umbilical cord matrix-derived mesenchymal stem cells into germ-like cells. Avicenna J Med Biotechnol. 2014;6(4):218–227.
[12] Hsieh J-Y, Fu Y-S, Chang S-J, et al. Functional module analysis reveals differential osteogenic and stemness potentials in human mesenchymal stem cells from bone marrow and Wharton's Jelly of Umbilical Cord. Stem Cells Dev. 2010;19(12):1895–1910.
[13] Wang L, Tran I, Seshareddy K, et al. A comparison of human bone marrow–derived mesenchymal stem cells and human umbilical cord–derived mesenchymal stromal cells for cartilage tissue engineering. Tissue Eng Part A. 2009;15(8):2259–2266.
[14] Paduszyński P, Aleksander-Konert E, Zajdel A, et al. Changes in expression of cartilaginous genes during chondrogenesis of Wharton's jelly mesenchymal stem cells on three-dimensional biodegradable poly (L-lactide-co-glycolide) scaffolds. Cell Mol Biol Lett. 2016;21(1):14.
[15] Jamalpoor Z, Taromi N, Soleimani M, et al. In vitro interaction of human Wharton's jelly mesenchymal stem cells with biomimetic 3D scaffold. J Biomed Mater Res A. 2019;107(6):1166–1175.
[16] Hosseini S, Vasaghi A, Nakhlparvar N, et al. Differentiation of Wharton's jelly mesenchymal stem cells into neurons in alginate scaffold. Neural Regen Res. 2015;10(8):1312–1316.
[17] Gauthaman K, Venugopal JR, Yee FC, et al. Osteogenic differentiation of human wharton's jelly stem cells on nanofibrous substrates in vitro. Tissue Eng Part A. 2010;17(1–2):71–81.
[18] Bagher Z, Ebrahimi-Barough S, Azami M, et al. Cellular activity of Wharton's Jelly-derived mesenchymal stem cells on electrospun fibrous and solvent-cast film scaffolds. J Biomed Mater Res A. 2016;104(1):218–226.
[19] Novoselov KS, Geim AK, Morozov SV, et al. Electric field effect in atomically thin carbon films. Science. 2004;306(5696):666–669.
[20] Editorial. *It's still all about graphene*. Nat Mater. 2010;10:1.
[21] Choi W, Lahiri I, Seelaboyina R, et al. Synthesis of graphene and its applications: a review. Critl Rev Solid State Mater Sci. 2010;35(1):52–71.
[22] Potts JR, Dreyer DR, Bielawski CW, et al. Graphene-based polymer nanocomposites. Polymer. 2011;52(1):5–25.
[23] Liu J, Cui L, Losic D. Graphene and graphene oxide as new nanocarriers for drug delivery applications. Acta Biomater. 2013;9(12):9243–9257.
[24] Wate PS, Banerjee SS, Jalota-Badhwar A, et al. Cellular imaging using biocompatible dendrimer-functionalized graphene oxide-based fluorescent probe anchored with magnetic nanoparticles. Nanotechnology. 2012;23(41):415101.
[25] Depan D, Girase B, Shah JS, et al. Structure–process–property relationship of the polar graphene oxide-mediated cellular response and stimulated growth of osteoblasts on hybrid chitosan network structure nanocomposite scaffolds. Acta Biomater. 2011;7(9):3432–3445.
[26] Depan D, Shah J, Misra RDK. Controlled release of drug from folate-decorated and graphene mediated drug delivery system: synthesis, loading efficiency, and drug release response. Mater Sci Eng C. 2011;31(7):1305–1312.
[27] Kim J, Choi KS, Kim Y, et al. Bioactive effects of graphene oxide cell culture substratum on structure and function of human adipose-derived stem cells. J Biomed Mater Res A. 2013;101(12):3520–3530.
[28] Marcela D, Patricia FA, Nelson D, et al. Graphene oxide sheets-based platform for induced pluripotent stem cells culture: toxicity, adherence, growth and application. J Phys. 2015;617(1):012021.

[29] Garcia-Alegria E, Iliut M, Stefanska M, et al. Graphene Oxide promotes embryonic stem cell differentiation to haematopoietic lineage. Sci Rep. 2016;6:25917.
[30] Halim A, Luo Q, Ju Y, et al. A mini review focused on the recent applications of graphene oxide in stem cell growth and differentiation. Nanomaterials. 2018;8(9):736.
[31] Puah PY, Moh PY, Lee PC, et al. Spin-coated graphene oxide as a biomaterial for Wharton's Jelly derived mesenchymal stem cell growth: a preliminary study. Mater Technol. 2018;33(13):835–843.
[32] He HX, Liu HC. Stem cell behaviours and functions modulated by biomaterials. Mater Technol. 2010;25 (3–4):231–236.
[33] Bajpai I, Rukini A, Jung K-J, et al. Surface morphological influence on the in vitro bioactivity and response of mesenchymal stem cells. Mater Technol. 2017;32 (9):535–542.
[34] Puah PY. ID2015 Preparation of graphene oxide/oligopeptides composite for promoting mesenchymal stem cell proliferation. Biomed Res Therapy. 2017;4 (S):S48–S48.
[35] Rosa V, Xie H, Dubey N, et al. Graphene oxide-based substrate: physical and surface characterization, cytocompatibility and differentiation potential of dental pulp stem cells. Dent Mater. 2016;32(8):1019–1025.
[36] Nguang SY, Wong SR, Law JS, et al. Enhancing adsorption property of Engelhard Titanosilicate-10 through incorporation of graphene oxide. Microporous Mesoporous Mater. 2017;252:125–139.
[37] Krueger M, Berg S, Stone D, et al. Drop-casted self-assembling graphene oxide membranes for scanning electron microscopy on wet and dense gaseous samples. ACS Nano. 2011;5(12):10047–10054.
[38] Kim F, Cote LJ, Huang J. Graphene oxide: surface activity and two-dimensional assembly. Adv Mater. 2010;22(17):1954–1958.
[39] Wei CB, Liu ZF, Jiang FF et al. Cellular behaviours of bone marrow-derived mesenchymal stem cells towards pristine graphene oxide nanosheets. Cell Prolif. 2017;50(5):e12367.
[40] Lee WC, Lim CHYX, Shi H, et al. Origin of enhanced stem cell growth and differentiation on graphene and graphene oxide. ACS Nano. 2011;5(9):7334–7341.
[41] Wang H-S, Hung S-C, Peng S-T, et al. Mesenchymal stem cells in the Wharton's Jelly of the human umbilical cord. Stem Cells. 2004;22 (7):1330–1337.
[42] Zhu W, Chen J, Cong X, et al. Hypoxia and serum deprivation-induced apoptosis in mesenchymal stem cells. Stem Cells. 2006;24(2):416–425.
[43] Ling YS, Lim LR, Yong YS, et al. MS-based metabolomics revealing Bornean Sinularia sp. extract dysregulated lipids triggering programmed cell death in Hepatocellular carcinoma. Nat Prod Res. 2018;1–8.
[44] Ryoo S-R, Kim Y-K, Kim M-H, et al. Behaviors of NIH-3T3 fibroblasts on graphene/carbon nanotubes: proliferation, focal adhesion, and gene transfection studies. ACS Nano. 2010;4(11):6587–6598.
[45] Kang E-S, Song I, Kim D-S, et al. Size-dependent effects of graphene oxide on the osteogenesis of human adipose-derived mesenchymal stem cells. Colloids Surf B Biointerfaces. 2018;169:20–29.
[46] Faghihi S, Azari F, Zhilyaev AP, et al. Cellular and molecular interactions between MC3T3-E1 pre-osteoblasts and nanostructured titanium produced by high-pressure torsion. Biomaterials. 2007;28(27):3887–3895.
[47] Girase B, Shah JS, Misra RDK. Cellular mechanics of modulated osteoblasts functions in graphene oxide reinforced elastomers. Adv Eng Mater. 2012;14(4): B101–B111.
[48] Wang Y, Lee WC, Manga KK, et al. Fluorinated graphene for promoting neuro-induction of stem cells. Adv Mater. 2012;24(31):4285–4290.
[49] Qi W, Yuan W, Yan J, et al. Growth and accelerated differentiation of mesenchymal stem cells on graphene oxide/poly-l-lysine composite films. J Mat Chem B. 2014;2(33):5461–5467.
[50] Kawamoto K, Miyaji H, Nishida E, et al. Characterization and evaluation of graphene oxide scaffold for periodontal wound healing of class II furcation defects in dog. Int J Nanomedicine. 2018;13:2365.
[51] Yang Y, Wang X, Wang Y, et al. Influence of cell spreading area on the osteogenic commitment and phenotype maintenance of mesenchymal stem cells. Sci Rep. 2019;9(1):6891.
[52] Depan D, Pesacreta TC, Misra RDK. The synergistic effect of a hybrid graphene oxide–chitosan system and biomimetic mineralization on osteoblast functions. Biomater Sci. 2014;2(2):264–274.